

POWER-SPECTRUM ANALYSES OF THE GALLEX AND GNO SOLAR NEUTRINO DATA

By P.A. Sturrock¹, and D.O. Caldwell²

ADDRESSES

¹ Center for Space Science and Astrophysics, Varian 302, Stanford University, Stanford, California 94305-4060

² Physics Department, University of California, Santa Barbara, CA 93106-9530

(Received:)

ABSTRACT

Pandora has recently analyzed the Gallex-GNO dataset and finds no evidence for rotational modulation, in apparent contradiction of our earlier analyses. We have therefore re-analyzed Gallex and GNO data and examined the significance of different choices one may make in such analyses: (1) One may combine the Gallex and GNO data or analyze them by solar cycle; (2) One may use the Lomb-Scargle method or a likelihood method; (3) One may make significance estimates by means of Monte-Carlo simulations or by means of the shuffle procedure; (4) One may use a wide search band that is not related to solar rotation or a narrow search band that focuses on solar rotation; and (5) One may look for modulation at a single frequency or at a harmonically related pair of frequencies. We find that different choices yield different results. Whereas Pandora's choices yield no significant evidence for variability, other choices yield strong evidence for rotational modulation, one case leading to a significance level of 99.93%.

PACS Numbers: 14.60.Pq, 26.65.+t, 95.85.Ry, 96.40.Tv.

1. INTRODUCTION

In earlier articles [1-5], we have presented evidence for variability of the solar neutrino flux as measured by the Gallex [6 - 10] and GNO [11, 12] experiments. More recently, we have presented evidence of variability [5, 13, 14] in data acquired by the Super-

Kamiokande experiment [15, 16]. Our analysis of the Super-Kamiokande data has been criticized by the Super-Kamiokande collaboration [17], to which we have responded [18, 19].

Pandola [20] has recently presented an analysis of the combined Gallex-GNO dataset, which he claims “does not support the presence of a time variability with characteristic periods resembling those of rotation of the solar magnetic fields....” The purpose of this article is to re-analyze the Gallex and GNO data in order (a) to shed light on the origin of the discrepancy between the different conclusions drawn by Pandola and by us, and (b) to re-assess the evidence for rotational modulation.

The answer one obtains from an exercise in scientific research depends sharply on the precise formulation of the question being addressed. If two analyses involve different formulations of what is intended to be the same question, it should not be surprising if the answers turn out to be different.

Pandola carried out analyses of the merged Gallex and GNO data (although he comments briefly on an analysis of GNO data). We shall compare the results of an analysis of the combined data, and of separate analyses of the Gallex and GNO datasets. We have found in the past [5] (and we confirm in this investigation) that evidence for rotational modulation is concentrated in the solar cycle in which the Gallex dataset was taken. Hence, after this initial review, we concentrate on Gallex data.

We next consider different methods of power-spectrum analysis. Pandola’s basic procedure is to apply the Lomb-Scargle method [21, 22], assigning flux measurements to the end-time $t_{e,r}$ of each run r ($r = 1, \dots, R$). We repeat this analysis, but we also consider a modification of a likelihood analysis, first used [23] in our study of Homestake data [24], that takes account of both the start time $t_{s,r}$ and end time of each run. We consider that the latter procedure is to be preferred over the former, since it takes into account more of the available experimental data. (Pandola also presents the results of a maximum-likelihood analysis. We comment on this briefly in Section 6.)

In assessing the statistical significance of a peak in the power spectrum, Pandola examines the probability of finding a peak of that strength or more by chance in a search band that he chose to be 0 to 26 yr^{-1} in a set of Monte-Carlo simulations. This involves two assumptions to which there are alternatives. Monte-Carlo simulations, as carried out by Pandola, are based on the assumption that the appropriate probability distribution function for flux measurements is normal, with half-width given by the standard deviation of the measurements. However, the distribution of flux measurements does not fit a normal distribution, so this assumption is not appropriate for the analysis of Gallex-GNO data. An alternative procedure, which does not rest on any assumption about the form of the distribution of flux measurements, is the shuffle procedure by which one randomly reassigns flux measurements and timing data. We find that the shuffle procedure leads to sharper significance estimates than Monte Carlo simulations.

The second point raised in the previous paragraph is that a search band of width 0 to 26 yr^{-1} may be appropriate if one has no idea what frequency may play a role in the modulation of the solar neutrino flux. However, we have drawn attention to the possibility that the solar neutrino flux may be influenced by internal magnetic structures that co-rotate with some region of the solar interior, and Pandola refers specifically to “time variability with characteristic periods resembling those of rotation of the solar magnetic fields...” For this specific hypothesis, the appropriate search band is much smaller than that adopted by Pandola. Based on our examination of helioseismology data [25], we consider that an appropriate search band is 13.4 to 14.9 yr^{-1} sidereal frequency (as it would be detected from a platform fixed in space), or 12.4 to 13.9 yr^{-1} synodic frequency (as it would be detected on Earth). This more restricted search band leads of course to a substantial change in significance estimates.

If the flux modulation (assumed real) is stable and strictly sinusoidal, one would expect to find a single peak in the power spectrum. However, if the modulation is periodic and stable but not sinusoidal, one may find peaks corresponding to harmonics of the fundamental, as well as one due to the fundamental itself. We therefore examine not only the

distribution of powers of a single peak, but also the distribution of the sum of powers corresponding to a fundamental and the lowest (usually termed the “second”) harmonic.

Pandola’s negative result came from (a) choosing to combine the Gallex and GNO data, (b) using the Lomb-Scargle method of power spectrum analysis, (c) adopting a very wide search band, (d) using Monte-Carlo simulations, implicitly assuming the distribution of the flux measurements to be normal, and (e) considering the power in a single peak. We show that by (a) analyzing Gallex data only, (b) using a likelihood method of power-spectrum analysis, (c) adopting a search band tailored to a search for rotational modulation, and (d) using the shuffle test, that uses the actual distribution of flux measurements, one obtains strong evidence in support of rotational modulation. By also (e) combining the powers at two frequencies in 2:1 ratio, one obtains yet stronger evidence for such modulation.

2. LOMB-SCARGLE POWER-SPECTRUM ANALYSIS

From any series of measurements x_r at times t_r , where $r = 1, \dots, R$, we may form a power spectrum by the method developed by Lomb [21] and by Scargle [22]. From the flux measurements g_r , we form the variable x_r that has mean value zero:

$$x_r = g_r - \text{mean}(g). \quad (2.1)$$

The power spectrum $S(\nu)$ is then given by

$$S(\nu) = \frac{1}{2\sigma_0^2} \left\{ \frac{\left[\sum_r x_r \cos(2\pi\nu(t_r - \tau)) \right]^2}{\left[\sum_r \cos^2(2\pi\nu(t_r - \tau)) \right]} + \frac{\left[\sum_r x_r \sin(2\pi\nu(t_r - \tau)) \right]^2}{\left[\sum_r \sin^2(2\pi\nu(t_r - \tau)) \right]} \right\}, \quad (2.2)$$

where

$$\sigma_0 = \text{std}(x_r), \quad (2.3)$$

and τ is defined by the relation

$$\tan(4\pi\nu\tau) = \frac{\sum_r \sin(4\pi\nu t_r)}{\sum_r \cos(4\pi\nu t_r)}. \quad (2.4)$$

In order to use the Lomb-Scargle procedure, it is necessary to assign a definite time t_r to each run. In agreement with Pandola [20], we adopt the end-time as a convenient choice. Using the 65 runs of the Gallex dataset, we obtain the power-spectrum shown in Figure 1 that shows a peak with power $S = 7.33$ and frequency 13.64 yr^{-1} , which falls within the frequency band of the equatorial solar internal rotation (12.4 to 13.9 yr^{-1} [25]. Using all 123 runs of the Gallex-GNO dataset analyzed by Pandola, we obtain the power-spectrum shown in Figure 2. There is a peak at almost the same frequency, 13.63 yr^{-1} , but the power is now reduced to $S = 5.09$.

In order to understand the difference between Figures 1 and 2, it is convenient to form the “running power,” again formed by the Lomb-Scargle procedure. We evaluate the power first from runs 1 and 2, then from runs 1, 2, and 3, etc., ending with runs 1 through 123. When we evaluate the power spectrum for the frequency 13.64 yr^{-1} , the result is as shown in Figure 3. We see that the power at this frequency builds up during the Gallex interval (1991.3 to 1997.1), but declines during the GNO interval (1998.4 to 2003.3). A Lomb-Scargle power spectrum for the GNO dataset alone is shown in Figure 4. The strongest peak in the rotational frequency range now occurs at frequency 13.78 yr^{-1} , with power only 2.46. The evidence for rotational modulation has virtually disappeared.

This result is consistent with the modulation properties of the solar neutrino flux depending upon the solar cycle. The Gallex interval falls within Solar Cycle 22, that began with the minimum 1986.8, reached a maximum in 1989.6, and ended with the minimum at 1996.8. By contrast, the GNO interval falls within Solar Cycle 23. The explanation [5] of the flux variability is that there is a Resonant-Spin-Flavor Precession (RSFP) of the solar neutrinos which is subdominant to the large-mixing-angle (see, for instance, [26]) MSW [27-30] transition. This RSFP process occurs in the convection zone of the Sun, and it is well

known that the convection zone magnetic field changes with solar cycle. For this reason, we consider only the Gallex dataset in the remainder of this article.

3. LIKELIHOOD POWER-SPECTRUM ANALYSIS

We now carry out power spectrum analysis, using a likelihood procedure similar to that introduced [23] for analysis of Homestake data [24]. Using the notation of Section 2, the log-likelihood that the data may be fit to a model that gives X_r as the expected values of x_r is given by

$$L = -\frac{1}{2} \sum_{r=1}^R (x_r - X_r)^2 / \sigma_r^2. \quad (3.1)$$

We estimate the power spectrum from the increase in the log-likelihood over the value expected for no modulation, corresponding to $X_r = 0$:

$$S = \frac{1}{2} \sum_{r=1}^R \frac{x_r^2}{\sigma_r^2} - \frac{1}{2} \sum_{r=1}^R \frac{(x_r - X_r)^2}{\sigma_r^2}. \quad (3.2)$$

Since the error estimates are highly variable and asymmetric, we simplify the analysis by adopting the standard deviation σ_0 of the measurements as the error terms, for all runs.

If we examine the possibility that the flux varies sinusoidally with frequency ν , and take account of the decay of neutrino-capture-produced atoms, the expected normalized flux estimates will be given by

$$X_r = \frac{1}{D_r} \int_{t_{sr}}^{t_{er}} dt (A e^{i2\pi\nu t} + A * e^{-i2\pi\nu t}) e^{-k_D(t_{er}-t)}, \quad (3.3)$$

where

$$D_r = t_{er} - t_{sr}. \quad (3.4)$$

For each frequency, the complex amplitude A is adjusted to maximize the likelihood.

The resulting power spectrum is shown in Figure 5. We see that the height of the peak at 13.64 yr^{-1} has now increased to 7.81.

4. SIGNIFICANCE ESTIMATES

We may carry out preliminary significance estimates by using the “false-alarm” formula [22]:

$$P = 1 - (1 - e^{-S})^M, \quad (4.1)$$

where M is the number of “independent frequencies” for the search band under consideration. We may estimate M empirically by examining the power spectrum shown in Figure 5. We find that there are 119 peaks in the band 0 to 26 yr^{-1} , but only 8 in the band 12.4 to 13.9 yr^{-1} . Hence, with the value $S = 7.81$, we find that there is a probability of 4.7% of obtaining a peak that big or bigger in the band 0 to 26 yr^{-1} , but a probability of only 0.32% of obtaining a peak that big or bigger in the range 12.4 to 13.9 yr^{-1} .

We now carry out significance estimates by the Monte Carlo procedure [19], as used by Pandola [20] in his analysis of Gallex-GNO data. We generate a large number of simulated datasets by the algorithm

$$x_{MC,r} = \sigma_0 \text{randn}, \quad (4.2)$$

where randn is the operation of producing random numbers with a normal distribution and variance unity. For each fictitious dataset, we compute the power spectrum over the search band, we note the power SM of the biggest peak, and we then examine the distribution of the maximum-power values. This distribution is shown in Figure 6 for the band 0 to 26 yr^{-1} , and in Figure 7 for the band 12.4 to 13.9 yr^{-1} . We find that, for the band 0 to 26 yr^{-1} , 1379 of 10,000 simulations have maximum power of 7.81 or more, giving a significance level of 86%; for the band 12.4 to 13.9 yr^{-1} , 124 of 10,000 simulations have maximum power of 7.81 or more, giving a significance level of 99 %. These significance estimates are weaker than those expected from our calculation of the false-alarm probabilities.

However, we should note that the Monte Carlo simulations are based on the implicit assumption that the flux measurements are drawn from a normal distribution. Inspection of the data shows that this is a poor assumption. The actual distribution is highly asymmetric, and has more high values than one would expect from a normal distribution. For this reason, it is preferable to adopt the shuffle test, which works with the actual flux distribution rather

than an assumed distribution. For each simulation, the flux values are randomly re-assigned to the timing data. For each set of shuffled data, we compute the power spectrum over the search band, we note the power SM of the biggest peak, and we then examine the distribution of the maximum-power values. This distribution is shown in Figure 8 for the band 0 to 26 yr^{-1} , and in Figure 9 for the band 12.4 to 13.9 yr^{-1} . We find that, for the band 0 to 26 yr^{-1} , 518 of 10,000 simulations have maximum power of 7.81 or more, giving a significance level of 95%; for the band 12.4 to 13.9 yr^{-1} , 33 of 10,000 simulations have maximum power of 7.81 or more, giving a significance level of 99.7 %. These significance estimates are quite close to those expected from our calculation of the false-alarm probabilities.

It is interesting to compare the shapes of the reverse cumulative distributions obtained by the Monte Carlo simulations and by the shuffle procedure. By comparing Figures 6 and 8 for the search band 0 to 26 yr^{-1} , we see that the former yields a power of 16.60, whereas the latter yields a maximum power of only 11.10. For the band 12.4 to 13.9 yr^{-1} , the figures are 12.47 and 9.52, respectively. This change of shape of the distribution helps explain why the shuffle test leads to higher significance levels than does the Monte Carlo process. Since the shuffle test makes no assumption concerning the distribution of flux measurements, it is to be preferred over Monte Carlo simulations.

5. FUNDAMENTAL AND HARMONIC

On inspecting the power spectrum shown in Figure 5, we find that, in addition to the peak at 13.64 yr^{-1} with power 7.81, there is a peak at 27.32 yr^{-1} with power 5.03. These frequencies are in very close to a 2:1 ratio. There is no reason to expect that rotational modulation will yield a pure sinusoidal modulation, so it should not be surprising if we find evidence for modulation at the fundamental frequency and also at a low harmonic (in this case, the so-called “second” harmonic). In order to examine this possibility systematically, we search the Gallex dataset for all pairs of frequencies in a 2:1 ratio.

One procedure would be to form the sum of the powers at frequencies ν and 2ν :

$$Z(\nu) = S(\nu) + S(2\nu). \quad (5.1)$$

However, we have shown elsewhere [31] that the following function of Z , which we refer to as the “combined power statistic” (CPS), has the same distribution (exponential) as S :

$$G = Z - \log(1 + Z) . \quad (5.2)$$

This quantity is shown as a function of frequency in Figure 10. We find that there is a notable peak at frequency 13.65 yr^{-1} with value $G = 9.56$.

We may use the “false-alarm” formula to obtain significance estimates of this feature. For the band 0 to 26 yr^{-1} , we found that $M = 119$, leading to a false-alarm probability of 0.0084 (significance level 99.2%). For the band 12.4 to 13.9 yr^{-1} , we found that $M = 8$, leading to a false-alarm probability of 0.00056 (significance level 99.94%).

We have also obtained significance estimates by the shuffle procedure. For each set of shuffled data, we again compute the power spectrum over the search band, form the combined power statistic, note the value GM of the biggest peak, and examine the distribution of the maximum-CPS values. This distribution is shown in Figure 11 for the band 0 to 26 yr^{-1} , and in Figure 12 for the band 12.4 to 13.9 yr^{-1} . We find that, for the band 0 to 26 yr^{-1} , 79 of 10,000 simulations have a CPS value of 9.56 or more, giving a significance level of 99.2% ; for the band 12.4 to 13.9 yr^{-1} , 7 of 10,000 simulations have a CPS value of 9.56 or more, giving a significance level of 99.93% . These significance estimates are quite close to those expected from our calculation of the false-alarm probabilities.

6. DISCUSSION

As we stated in the introduction, the purpose of this article is to re-analyze the Gallex and GNO data in order (a) to shed light on the discrepancy between the different conclusions drawn by Pandola [20] and our previous work [1 – 5], and (b) to re-assess the evidence for rotational modulation. Concerning the former, we find that the difference may be attributed to different choices in the analysis procedure:

- Pandola analyzes the Gallex and GNO data taken together, whereas we separate the two datasets according to solar cycle, and then concentrate on the Gallex data.

- Pandola uses the Lomb-Scargle method of power-spectrum analysis, whereas we use a likelihood method.
- Pandola uses a very wide search band, which is not related to a search for rotational modulation. We use the same search band, but we also use a narrower band that we consider to be more appropriate for a search for rotational modulation.
- Pandola uses Monte-Carlo simulations for significance estimation, whereas we find that the shuffle test is more appropriate.
- Pandola examines the power spectrum, but we also examine the combined power statistic formed by combining powers at the “fundamental” rotation frequency and also at the harmonic of that frequency.

Concerning evidence for rotational modulation, we find that our re-analysis yields much stronger evidence than our previous articles. This difference may be attributed to the choices specified above. None of our earlier relevant articles [1 – 5] makes all of these choices, although article [1] analyzed Gallex data only, and articles [3] and [4] used the shuffle test, applied to a narrow search band. When all of the factors listed above are taken into account, we find that the evidence for rotational modulation is significant at a level better than 99.9%.

Finally, we comment on the maximum-likelihood analysis of Pandola [20, Section 3]. This analysis differs from our analysis in that Pandola effectively uses a three-parameter fit to the data (n_0, A , and ϕ , in his notation). This is equivalent to the three-parameter fit used by Koshio [32] in his analysis of Super-Kamiokande data. We have found that this approach (the “floating offset method”) leads to ill-conditioned equations, producing erratic amplitude and offset estimates [19]. In the analysis of Super-Kamiokande data, significance estimates made by the floating-offset method reach lower significance levels than estimates made by the two-parameter (complex amplitude) method. It is therefore not surprising that the same appears to be true in the analysis of Gallex-GNO data.

It is evident that there are a number of choices to be made in searching for evidence of variability of the solar neutrino flux. If two investigators make different choices, we

should not be surprised if they get different answers. It then becomes necessary to scrutinize the choices very carefully.

We wish to thank Luciano Pandola for generous and helpful communications, and our colleagues Jeffrey Scargle, Alexander Kosovichev, Guenther Walther, and Michael Wheatland for their interest and helpful discussions. This work was supported by NSF grant AST-0097128

REFERENCES

- [1] P.A. Sturrock, J.D. Scargle, G. Walther, and M.S. Wheatland, *Ap J (Letters)*, 523, L177 (1999).
- [2] P.A Sturrock and J.D. Scargle, *ApJ (Letters)* 550, L101 (2001).
- [3] P.A. Sturrock and M.A. Weber, *Astrophys. J.* 565, 1366 (2002).
- [4] P.A. Sturrock and M.A. Weber, "Multi-Wavelength Observations of Coronal Structure and Dynamics -- Yohkoh 10th Anniversary Meeting", *COSPAR Colloquia Series*, P.C.H. Martens and D. Cauffman (eds.), 323 (2002).
- [5] D.O. Caldwell and P.A. Sturrock, *hep-ph/0309191* (2003).
- [6] P. Anselmann et al., *Phys. Lett. B* 314, 445 (1993).
- [7] P. Anselmann et al., *Phys. Lett. B* 342, 440 (1995).
- [8] T.A. Kirsten et al., *Nucl. Phys. B (Proc. Suppl.)* 38, 68 (1995).
- [9] W. Hampel et al., *Phys. Lett. B* 388, 384 (1996).
- [10] W. Hampel et al., *Phys. Lett. B* 447, 127 (1999).
- [11] G. M. Altmann et al., *Phys. Lett. B* 490, 16 (2000).
- [12] T.A. Kirsten et al., *Nucl. Phys. B (Proc. Suppl.)* 118, 33 (2003).
- [13] P.A. Sturrock, *Astrophys. J.* 594, 1102 (2003).
- [14] P.A. Sturrock, *Astrophys. J.* 605, 568 (2004).
- [15] Y. Fukuda, et al. 2001, *Phys. Rev. Lett.* 86, 5651 (2001).
- [16] Y. Fukuda, et al., *Phys. Lett. B*, 539, 179 (2002).
- [17] J. Yoo et al., *Phys. Rev. D*, 68, 092002 (2003).
- [18] P.A. Sturrock, D.O. Caldwell, J. D. Scargle, G. Walther, and M. S. Wheatland, *hep-ph/0403246* (2004).

- [19] P.A. Sturrock, hep-ph/0408017 (2004, submitted to Phys. Rev.D).
- [20] L. Pandola, hep-ph/0406248 (2004, submitted to Elsevier Press).
- [21] N. Lomb, *Astrophys. and Space Science*, 39, 447 (1976).
- [22] J.D. Scargle, *Astrophys. J.*, 263, 835 (1982).
- [23] P.A. Sturrock, G. Walther, and M.S. Wheatland, *Astrophys. J.*, 491, 409 (1997).
- [24] B.T. Cleveland et al., *Astrophys. J.*, 496, 505(1998).
- [25] J. Schou et al., *Astrophys. J.*, 505, 390 (1998).
- [26] J.N. Bahcall, M.C. Gonzalez-Garcia, and C. Pena-Garay, *JHEP* 0302 009 (2003).
- [27] L. Wolfenstein, *Phys. Rev. D*17, 2369 (1978).
- [28] L. Wolfenstein, *Phys. Rev. D*20, 2634 (1979).
- [29] S.P. Mikheyev and A.Yu. Smirnov, *Sov. J. Nucl. Phys.* 42, 913 (1985);
- [30] S.P. Mikheyev and A.Yu. Smirnov, *Nuovo Cimento* 9C, 17 (1986).
- [31] P.A. Sturrock, J. D. Scargle, G. Walther, and M. S. Wheatland, astro-ph/0304148 (2003).
- [32] V. Koshio, *Proceedings of the Second International Workshop on Neutrino Oscillations in Venice* (editor Milla Baldo Ceolin), p. 49 (2003).

FIGURES

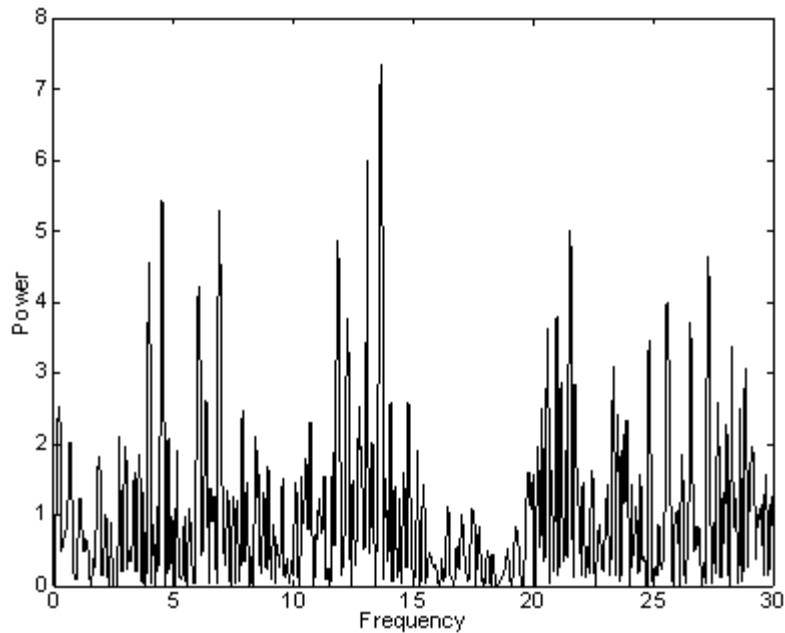


Figure 1. Lomb-Scargle power spectrum of the Gallex dataset.

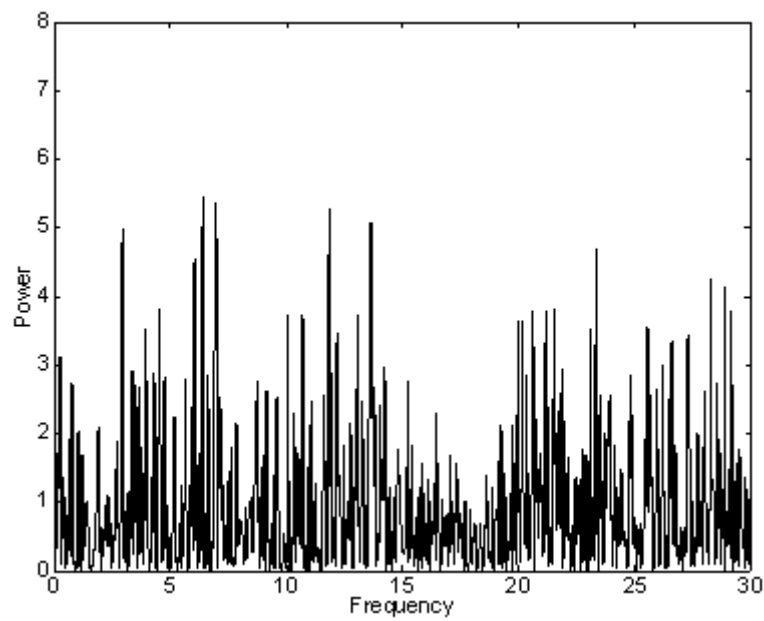


Figure 2. Lomb-Scargle power spectrum of the entire Gallex-GNO dataset.

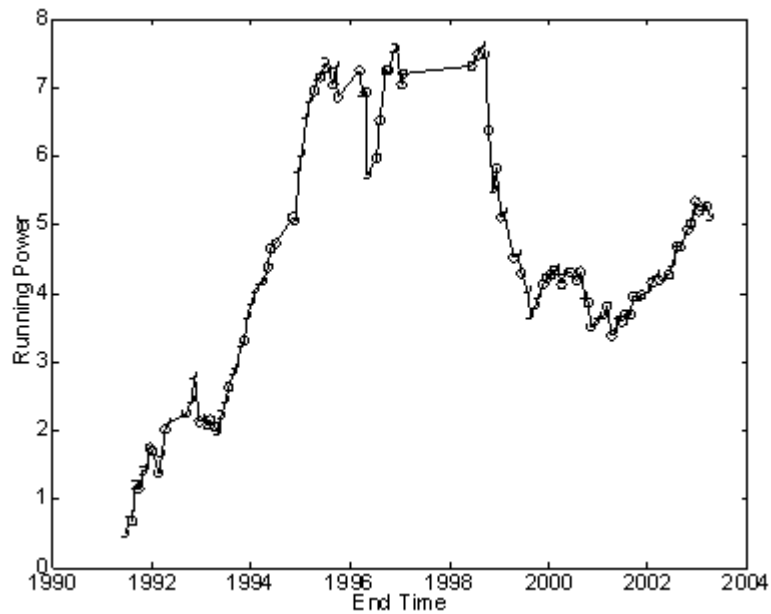


Figure 3. Running Rayleigh power, as a function of end time, for frequency 13.63 yr^{-1} from the Gallex-GNO data. Note that the power builds up during the Gallex time interval (1991.3 to 1997.1) that falls within Solar Cycle 22, but declines during the GNO time interval (1998.4 to 2003.3) that falls within Solar Cycle 23.

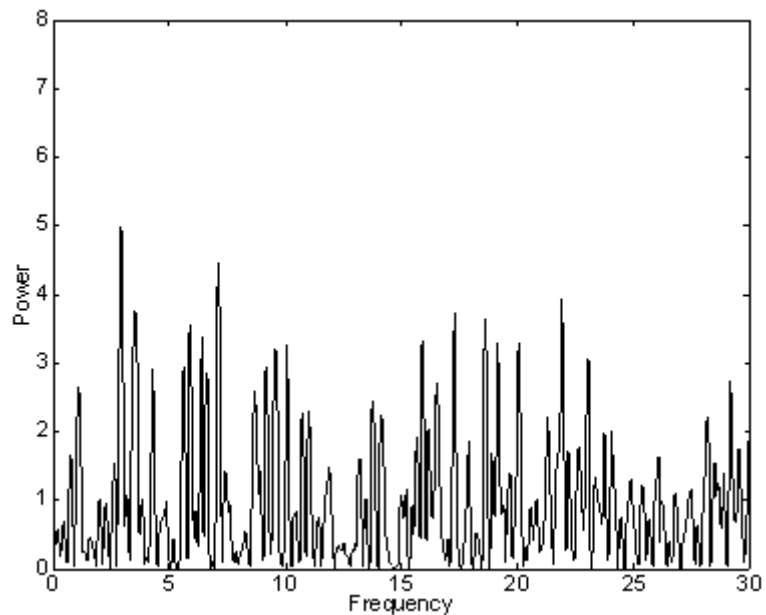


Figure 4. Lomb-Scargle power spectrum of the GNO dataset.

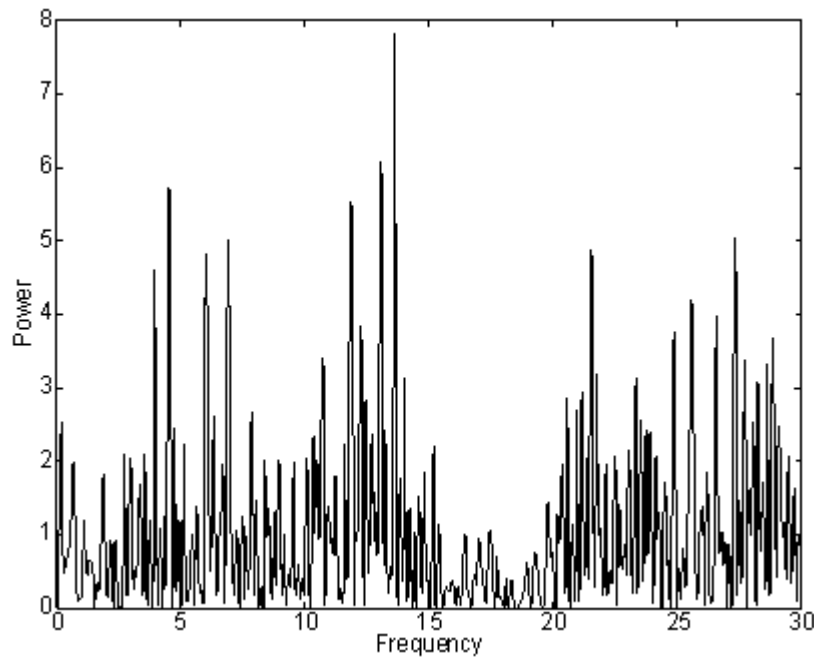


Figure 5. Likelihood power spectrum of the Gallex dataset.

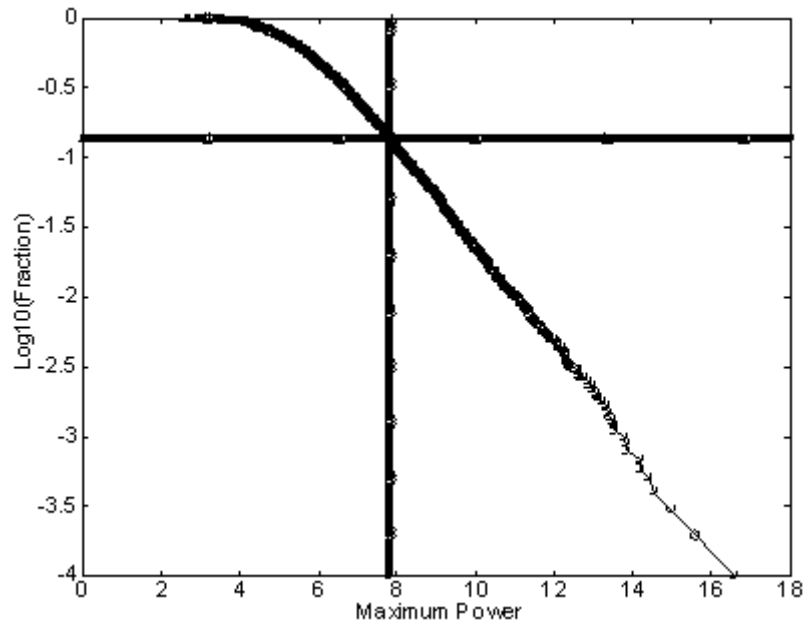


Figure 6. Reverse cumulative distribution of maximum power in the band 0 to 26 yr^{-1} , computed by Monte-Carlo simulations.

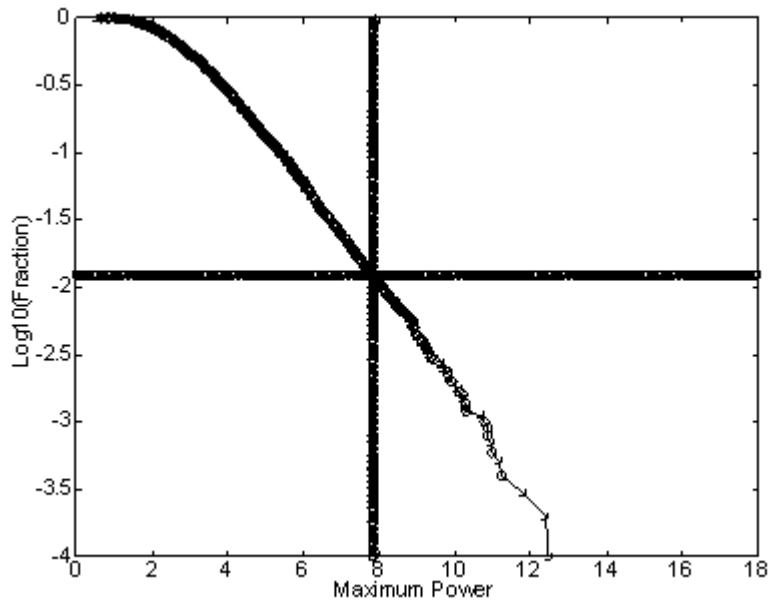


Figure 7. Reverse cumulative distribution of maximum power in the band 12.4 to 13.9 yr^{-1} , computed by Monte-Carlo simulations.

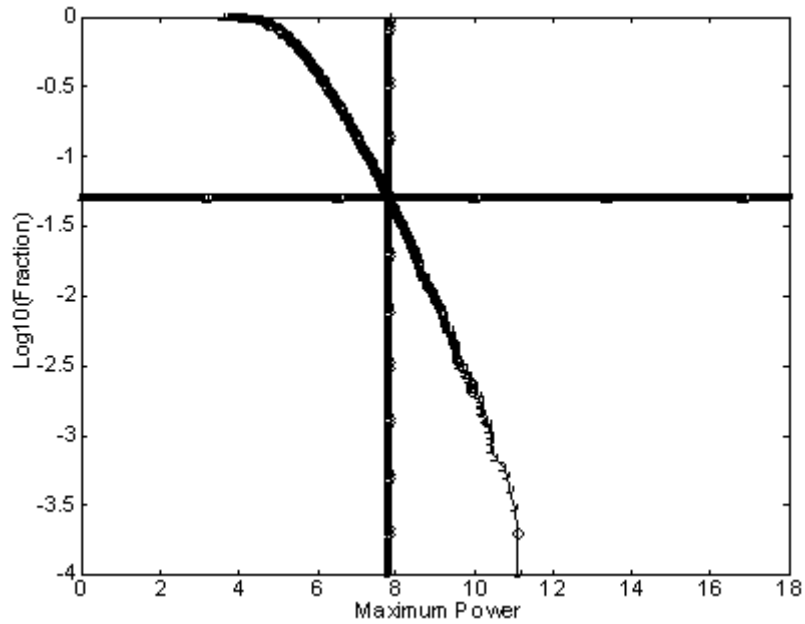


Figure 8. Reverse cumulative distribution of maximum power in the band 0 to 26 yr^{-1} , computed by shuffle simulations.

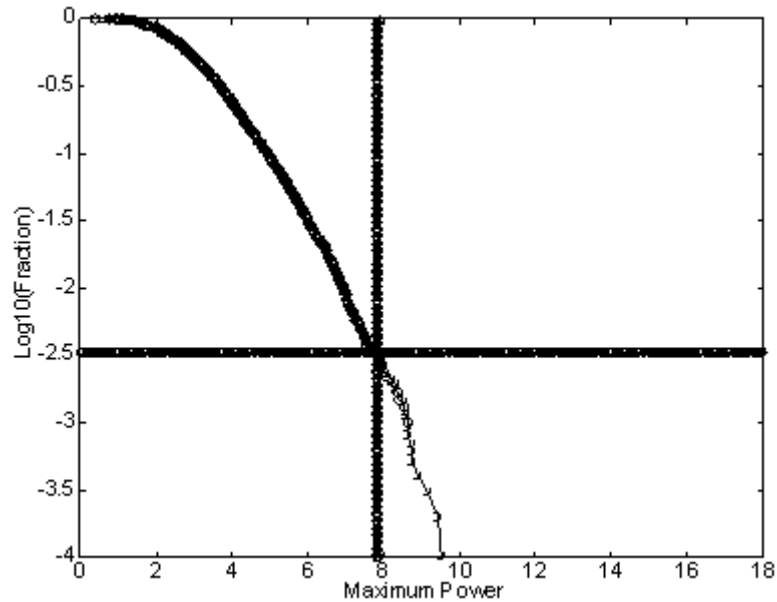


Figure 9. Reverse cumulative distribution of maximum power in the band 12.4 to 13.9 yr^{-1} , computed by shuffle simulations.

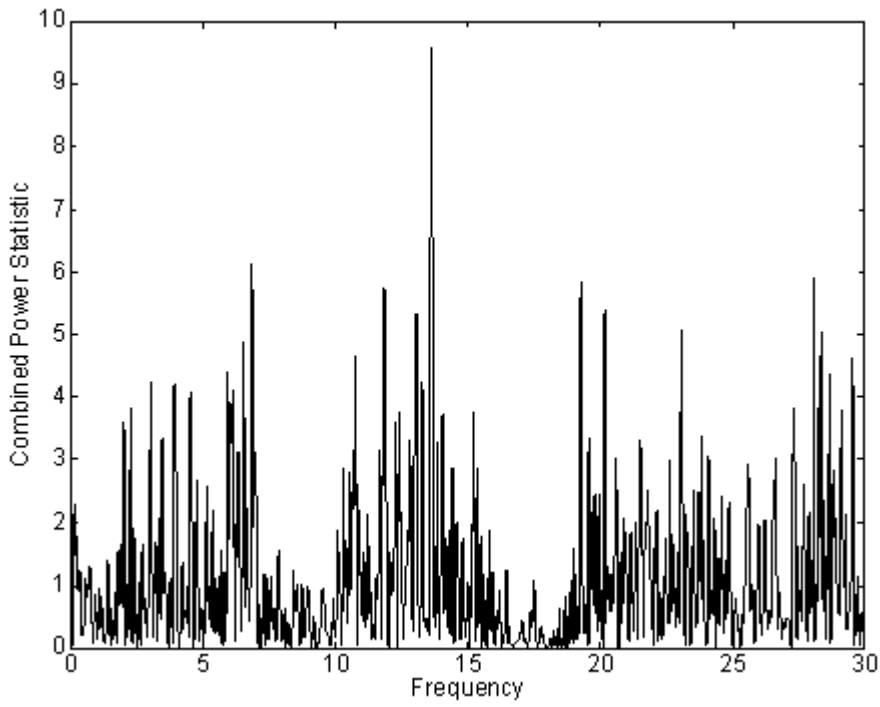


Figure 10. Combined power statistic, defined by equations (5.1) and (5.2), for the Gallex dataset.

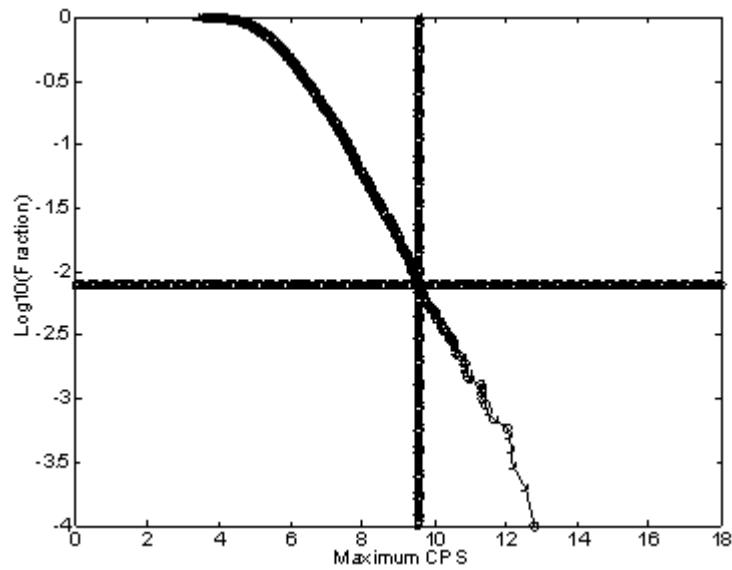


Figure 11. Reverse cumulative distribution of CPS values in the band 0 to 26 yr^{-1} , computed by shuffle simulations.

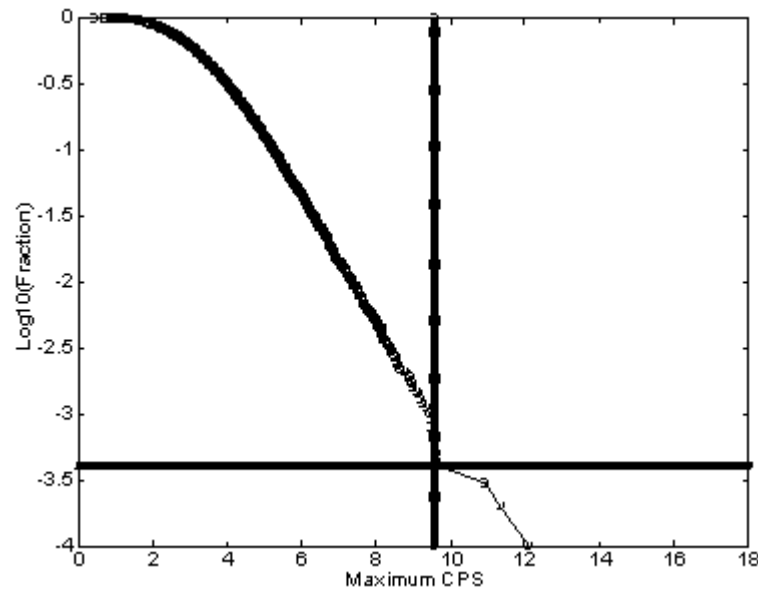


Figure 12. Reverse cumulative distribution of CPS values in the band 12.4 to 13.9 yr^{-1} , computed by shuffle simulations.